FEDSM2005-77421

DES, HYBRID RANS/LES AND PANS MODELS FOR UNSTEADY SEPARATED TURBULENT FLOW SIMULATIONS

D. Basu, A. Hamed and K. Das
Department of Aerospace Engineering and Engineering Mechanics
University of Cincinnati, Cincinnati, OH-45219

ABSTRACT

This paper presents computational results for two DES (Detached Eddy Simulation), one hybrid RANS (Reynolds Averaged Navier-Stokes)/ LES (Large Eddy Simulation) and some preliminary results from PANS (Partially Averaged Navier-Stokes) turbulence for simulation of unsteady separated turbulent flows. The models are implemented in a full 3-D Navier Stokes solver and are based on the two-equation k-ε model. The formulations of each model are presented and results are analyzed for subsonic flow over a Backward Facing Step (BFS). Simulations are carried out using a 3rd order Roe scheme. A comparative assessment is made between the predictions from the DES, hybrid and PANS models. The predicted results are compared with the available experimental data for skin-friction coefficient, and different turbulent quantities. The three-dimensionality of the flow field and the separated fine scale structures are presented through the Q iso-surfaces.

INTRODUCTION

Most of the numerical simulations for engineering applications at high Reynolds numbers are obtained using the RANS turbulence models. While RANS models yield prediction of useful accuracy in attached flows; they fail to accurately capture the complex flow structures in regimes substantially different from the thin shear and attached boundary layers. Simulation strategies such as LES are attractive as an alternative for prediction of flow fields where RANS is deficient but carry a prohibitive computational cost for resolving boundary layer turbulence at high Reynolds numbers. This in turn provides a strong incentive for the merging of these two techniques in DES, hybrid RANS-LES and PANS approaches.

DES [1,2,3] is a recently developed and the one of the most widely used hybridization technique for realistic simulations of high speed turbulent flows with massive separation. DES models were developed to combine the fine tuned RANS methodology in the attached boundary layers with the power of LES in the shear layers and separated flow regions at realistic Reynolds numbers [4,5]. It is a unified approach based on the adoption of a single turbulence model

that function as a sub-grid scale LES model in the separated flow regions where the grid is nearly isotropic and as a RANS model in attached boundary layers regions. It retains the essential features of LES type method as well as employs a computationally cheaper RANS method in regions where it is appropriate. This technique was originally designed to simulate massively separated flows and it provides better insight into the three-dimensional and time dependent flow features in comparison to the RANS models [6]. Spalart et al. [4] first proposed the concept of DES based on the original formulation of the Spalart-Allmaras (S-A) one-equation RANS model [7]. Subsequently, Strelets [5], Bush et al. [8], Batten et al. [9], Nichols et al. [10] proposed parallel concepts of DES based on two-equation turbulence models. Applications of the DES models for a wide variety of problems [11-15] involving separated flow configurations have shown certain degree of success relative to the RANS predictions. While DES is based on the adoption of a single turbulence model that functions as two different models (LES and RANS) in different regions, another class of hybridization technique relies on using two distinct turbulent models in the RANS and LES regions and is commonly known as the hybrid RANS/LES method. Georgiadis et al. [16] initiated the concept of explicit hybrid RANS/LES models by dividing the computational domain into RANS and LES regions. Baurle et al. [17] proposed another concept of hybrid technique that is based on a k-ω RANS and a sub-grid scale turbulent kinetic energy (SGS TKE) model. It relies on modifying the RANS TKE equations to a form that is consistent with the SGS TKE equation based on a blending function. Basu et al. [18] developed DES and hybrid models and applied them to transonic cavity flow and acoustic field simulations. They found that both the DES and hybrid models predicted the flow and acoustic fields in a similar fashion and increasing dissipation rate (ε) or decreasing turbulent kinetic energy (k) results in the same level of eddy viscosity in the DES formulations. Recently, Girimaji et al. [19] developed PANS (Partially Averaged Navier Stokes) based on the unresolved-to-total ratios of kinetic energy and dissipation. They have applied the PANS model for flow over a square cylinder, a

circular cylinder and nozzle flows and found the predictions to be quite encouraging [19].

In the present investigation, two DES formulations, one hybrid formulation and PANS formulation are analyzed for separated turbulent flows. The details of development for the DES and hybrid models, formulations and validation results for unsteady transonic cavity flows are provided in reference 18. The DES formulations are based on two-equation k- ε turbulence and the hybrid formulation is based on the combination [17] of the two-equation k-ε turbulence model [20] and a one-equation sub-grid-scale (SGS) model [21]. A blending function allows the SGS TKE equation to be triggered in the separated flow region and activates the RANS TKE equation in the attached flow region. The PANS model is in principle the same as developed by Girimaji et al. [19]. However, a spatially varying constant f_k is used for the current application. All the models are applied for the flow over a back-facing step (BFS). Turbulent flow over a backward facing step is a widely used validation problem to evaluate the performance of turbulence models in the prediction of massively separated flows. The separation and reattachment point of the flow, vortex size, fine scale structures, accuracy of predicted skin friction coefficient and different turbulent quantities provide a sensitive measure for the fidelity of the turbulence model. For the present investigation, simulation conditions for the BFS are adopted from the experimental study of Driver and Seegmiller [22] and the computed turbulent quantities from the DES models, hybrid model and PANS model are compared with the available experimental data [22].

METHODOLOGY

The governing equations for the present analysis are the full unsteady, three-dimensional compressible Navier-Stokes equations written in strong conservation-law form. They are numerically solved employing the implicit, approximate-factorization Beam-Warming algorithm [23]. Newton subiterations are used to improve temporal accuracy and stability properties of the algorithm. The aforementioned features of the numerical algorithm are codified in a parallel version of the time accurate three-dimensional solver FDL3DI, originally developed at AFRL [24]. It is a full three-dimensional parallel Navier stokes solver. In the Chimera based parallelization strategy [25], the computational domain is decomposed into a number of overlapped zones. In the solution process, each zone is assigned to a separate processor and communication between them is accomplished through the interpolation points in the overlapped region by explicit message passing using MPI libraries. The solver has been validated and proved to be efficient and reliable for a wide range of high speed and low speed; steady and unsteady problems [24-29]. In the present investigation, the 3rd order Roe scheme is used for the spatial discretization for both the flow and the turbulent equations. The time integration is carried out using the implicit Beam-Warming scheme with three subiterations for each time step. Turbulence is simulated by the DES and the hybrid RANS/LES models.

TURBULENCE MODELS

The DES models are based on the method of reducing the eddy viscosity (μ_t) in proportion to the local grid resolution, in the separated LES regions. This is achieved by modification and filtering of turbulent quantities that appear in the definition of the eddy viscosity. In this 1st DES formulation (DES1), the turbulent kinetic energy dissipation rate (ε) is increased to enable the transition from the RANS to LES type solution. In this 2nd DES formulation (DES2), the turbulent kinetic energy (k) is reduced to enable the transition from the RANS to LES type solution. These transitions are achieved through a limiter that is a function of the local turbulent length scale and the local grid dimensions. The hybrid model is a combination [17] of the RANS two-equation k-ε model [20] and the SGS one-equation model of Yoshizawa and Horiuti [21] using a blending function. The blending function relies on the local turbulent length scale and the local grid dimensions to enable the switching from the RANS equations to the SGS equations. The detailed formulations of the DES and the hybrid models are provided in reference 18. The PANS formulations are the same as given by Girimaji et al. [19]. The variable f_k used in the PANS equations has the form of $(\varepsilon * C_b * \Delta)^{2/3} / k$, where C_b is a floating coefficient (~ 0.5) and Δ is the local grid dimension. For the preliminary PANS simulations, a constant C_b of 0.5 is used.

NUMERICS

The computational domain for the BFS flow configuration is shown in figure 1 and consists of $327 \times 147 \times 80$ grids in the streamwise, wall normal and span-wise directions respectively. The simulations are carried out at a Reynolds number of 0.6×10^6/ft to optimize the available computational resources. This is lower than the experimental Reynolds number of 0.83×10^6/ft. The simulated Reynolds number ensures that the boundary layer is fully turbulent before passing over the step. The Mach number for the present simulations is 0.128. The backstep height (h) is 0.04 ft. The upstream length is 4h and the recirculation/separation region length is 24h. The expansion ratio is 1:10. The upper boundary is placed at 9h above the BFS opening. In the span-wise direction, the width is kept at 4h. Inflow data at the upstream boundary for the BFS were obtained from a separate flat plate simulation, which was used to produce profiles of the dependent variables. From the time-mean flowfield of the flat plate, a particular streamwise location was determined and the profile information was extracted. At that selected position, the boundary layer thickness is 1.4 times the BFS height ($\delta/H = 1.4$). This is approximately equal to the experimental value of δ ($\delta/H = 1.5$) at a location 4H upstream of the BFS lip (inflow plane) and the obtained velocity profile matched reasonably well with the experimental inflow velocity profile. In the upstream region, highly stretched RANS type grid is employed with 30 grid points within the boundary layer. The grid in the wall normal direction is clustered near the wall with a minimum grid spacing (Δy) of 7.5×10^{-4}h, which results in an y^+ value of 1 for the 1st grid point. At the inflow plane, the pressure is extrapolated from interior and the other flow variables were prescribed from the profile obtained from the flat plate simulations. The pressure at the outflow boundaries

was set equal to the free stream value and the other variables were extrapolated from the interior through a first order extrapolation. The top of the computational domain is set as inviscid / slip wall. In the span-wise direction, symmetric boundary conditions are applied. The simulations were initiated in the unsteady mode with a constant time step of 2.86×10^{-7} seconds. After the initial transients have been purged out, time averaging is applied over a sufficient long period of time. The solution domain is decomposed into thirteen overlapping zones in the stream-wise direction and the normal direction for parallel computation with a five-point overlap between the zones. Parallel computations for the overlapping zones for the BFS were performed using clustered Linux machines and exclusive message passing with MPI libraries. The zones were constructed in such a way that the load sharing among the processors was nearly equal.

RESULTS AND DISCUSSIONS

Computed results are presented for the turbulent quantities such as resolved turbulent kinetic energy and Reynolds stress profiles, velocity profiles, skin friction coefficient distribution and they are compared with available experimental data [22]. Vorticity field iso-surfaces are presented to illustrate the fine scale structures and three-dimensionality of the flowfield.

The computed boundary layer profile upstream of the BFS lip (X/H = 3.0) is compared to the well-known analytical expression of Spalding in figure 2(a) for the two DES models and the hybrid formulation. The results indicate that the computed boundary layer is fully turbulent for all three cases and is in agreement with Spalding's expression [30]. Figure 2(b) shows the comparison of the streamwise velocity profile at the same location with the experimental data. It clearly shows that all three turbulence models predicted similar upstream boundary layer profiles that are in reasonable agreement with the experimental data. However, the discrepancy near the boundary layer edge between the computed profile and the experimental data might be due to the difference in the simulated and the experimental Reynolds number. Figure 3 show the time-mean span-wise averaged skin friction coefficient distribution over the backward facing step for all the different turbulence models and their comparison with the experimental data. All the models predict the reattachment point a little upstream in comparison to the experimental reattachment location. The predicted skin friction coefficient values match quite well with the experimental results downstream of the reattachment. However, in the vicinity of the reattachment point, the predicted skin-friction coefficient is over-predicted and farther downstream, the coefficient is under-predicted. Figure 4 shows the comparison of the computed time-mean spanwise averaged grid resolved TKE profiles along with experimental data at three axial locations within the separated region. In general, the TKE profiles are comparable to the experimental data for all the models. At X/H = 5.5, the values are in reasonable agreement with the experiment. However, further downstream, the computed results deviate from the experimental observation. This might be due to the difference in the simulated and experimental Reynolds numbers. The

preliminary PANS also exhibit a pattern similar to the experimental results. Figure 5 compares the predicted time-mean spanwise averaged Reynolds stress ($u'v'$) profiles with the experimental data at three axial locations within the separated region. The computed Reynolds stress profiles also show trends similar to the resolved TKE; matching well with the experimental value at X/H = 5.5 and deviating further downstream. Figure 6 presents the comparison of the predicted time-mean spanwise averaged streamwise velocity distribution with the experimental data at three axial locations within the separated region. Even though there are some discrepancies between the experimental data and the computational results in the near wall region, the overall trend of the predictions is in good agreement with experimental findings.

Figure 7 presents the instantaneous iso-surfaces of the axial component of the quantity Q (Q_x) [31] to show the three-dimensionality of the flowfield, the formation of eddies within the separated region and also the evolution of the vortical structures. It clearly indicates the formation of the Kelvin-Helmholtz instabilities, the breakdown of the vortex as it is convected downstream and the associated formation of separated fine scale structures. The DES models as well as the hybrid RANS/LES model capture the shedding of the vortex downstream of the step and the subsequent helical pairing of the vortex sheets. Figure 8 presents the instantaneous iso-surfaces of the spanwise component of the quantity Q (Q_z). It can be observed that at the upstream region, the vortex sheet is essentially two-dimensional in nature but immediately after the flow expands into the separated region there is vortex breakdown, rapid stretching and the initiation of fine scale structures. Dubief et al. obtained similar results [32] for their LES simulations of BFS flow at a lower Reynolds numbers.

CONCLUSIONS

This paper presents numerical results for two DES models, one hybrid RANS/LES model and preliminary results for PANS model for high Reynolds number separated turbulent flow over a Backward Facing Step. Simulated results showed that the models have successfully captured the flow features in the separated region, including three-dimensionality of the flowfield, fine scale structures and turbulence quantities. Computed skin friction coefficient, resolved TKE and Reynolds stress profiles are in reasonable agreement with the experimental results. Observed discrepancies in the different profiles might be due to the difference in the simulated and the experimental Reynolds number. Preliminary results from the PANS simulations are encouraging; however further analysis is needed to determine the equivalence between the proposed models.

REFERENCES

1. Spalart, P. R., "Strategies for Turbulence Modeling and Simulations," 2000, International Journal of Heat and Fluid Flow, Vo. 21, pp. 252-263.
2. Hamed, A., Basu, D., and Das, K., "Detached Eddy Simulations of Supersonic Flow over Cavity," 2003, 41st AIAA Aerospace Sciences Meeting and Exhibit, Reno, Nevada, AIAA -2003-0549.
3. Sinha, N., Dash, S. M., Chidambaram, N. and Findlay, D., "A Perspective on the Simulation of Cavity Aeroacosutics", 1998, AIAA-98-0286.
4. Spalart, P. R., Jou, W. H., Strelets, M., and Allmaras, S. R., "Comments on the Feasibility of LES for Wings, and on a Hybrid RANS/LES Approach," 2001, First AFOSR International Conference on DNS/LES, Ruston, Louisiana, USA.
5. Strelets, M., "Detached Eddy Simulation of Massively Separated Flows", 2001, 39th AIAA Aerospace Sciences Meeting and Exhibit, AIAA-2001-0879.
6. Krishnan, V., Squires, K. D., Forsythe, J. R., "Prediction of separated flow characteristics over a hump using RANS and DES", 2004, AIAA-2004-2224.
7. Spalart, P. R., and Allmaras, S. R., " A one-equation turbulence model for aerodynamic flows", La Rech. A'reospatiale, 1994, Vol. 1, pp. 5-21.
8. Bush, R. H., and Mani, Mori, "A two-equation large eddy stress model for high sub-grid shear", 2001, 31st AIAA Computational Fluid Dynamics Conference, AIAA-2001-2561
9. Batten, P., Goldberg, U., and Chakravarthy, S., "LNS – An approach towards embedded LES", 2002, 40th AIAA Aerospace Sciences Meeting and Exhibit, AIAA-2002-0427.
10. Nichols, R. H., and Nelson, C. C., "Application of Hybrid RANS/LES Turbulence models", 2003, 41st AIAA Aerospace Sciences Meeting and Exhibit, Reno, Nevada, AIAA 2003-0083.
11. Travin, A., Shur, M., Strelets, M. and Spalart, P. R., "Detached-Eddy Simulations Past a Circular Cylinder," 1999, Flow Turbulence and Combustion, Vol. 63, pp. 293-313.
12. Constantinescu, G., Chapelet, M., Squires, K., "Turbulence Modeling Applied to Flow over a Sphere," 2003, AIAA Journal, Vol. 41, No. 9, pp. 1733-1742.
13. Hedges, L. S., Travin, A. K. and Spalart, P. R., "Detached-Eddy Simulations Over a Simplified Landing Gear," 2002, Journal of Fluids Engineering, Transaction of ASME, Vol. 124, No. 2, pp. 413-423.
14. Forsythe, J. R., Squires, K. D., Wurtzler, K. E., and Spalart, P. R., "Detached-Eddy Simulation of the F-15E at High Alpha", 2004, Journal of Aircraft, Vol. 41, No. 2, pp. 193-200.
15. Hamed, A., Basu, D., and Das, K., "Assessment of Hybrid Turbulence Models for Unsteady High Speed Separated Flow Predictions", 2004, 42nd AIAA Aerospace Sciences Meeting and Exhibit, Reno, Nevada, AIAA -2004-0684.
16. Georgiadis, N. J., Alexander, J. I. D., and Roshotko, E., "Hybrid Reynolds-Averaged Navier-Stokes/Large-Eddy Simulations of Supersonic Turbulent Mixing", 2003, AIAA Journal, Vol. 41, No. 2, pp. 218-229
17. Baurle, R. A., Tam, C. J., Edwards, J. R., and Hassan, H. A., "Hybrid Simulation Approach for Cavity Flows: Blending, Algorithm, and Boundary Treatment Issues", 2003, AIAA Journal, Vol. 41, No. 8, pp. 1463-1480.
18. Basu, D., Hamed, A., and Das, K., "DES and Hybrid RANS/LES models for unsteady separated turbulent flow predictions", 2005, AIAA-2005-0503.
19. Girimaji, Sharath S., Abdol-Hamid, Khaled S., "Partially –averaged Navier Stokes model for Turbulence: Implementation and Validation", 2005, AIAA-2005-0502.
20. Gerolymos, G. A., "Implicit Multiple grid solution of the compressible Navier-Stokes equations using k-ε turbulence closure", 1990, AIAA Journal, Vol. 28, No. 10, pp. 1707-1717.
21. Yoshizawa, A., and Horiuti, K., "A Statistically Derived Subgrid Scale Kinetic Energy Model for the Large-Eddy Simulation of Turbulent Flows", 1985, Journal of the Physical Society of Japan, Vol. 54, No. 8, pp. 2834-2839.
22. Driver, D.M. and Seegmiller, H.L., "Features of a Reattaching Turbulent Shear Layer in Divergent Channel Flow," AIAA Journal, Vol. 23, No. 2, Feb. 1985, pp. 163-171.
23. Beam, R., and Warming, R., "An Implicit Factored Scheme for the Compressible Navier-Stokes Equations," 1978, AIAA Journal, Vol. 16, No. 4, pp. 393-402.
24. Gaitonde, D., and Visbal, M. R., "High-Order Schemes for Navier-Stokes Equations: Algorithm and Implementation into FL3DI", 1998, AFRL-VA-TR-1998-3060.
25. Morgan, P. E., Visbal, M. R., and Tomko, K., "Chimera-Based Parallelization of an Implicit Navier-Stokes Solver with Applications", 2001, 39th Aerospace Sciences Meeting & Exhibit, Reno, NV, January 2001, AIAA Paper 2001-1088.
26. Morgan, P., Visbal, M., and Rizzetta, D., "A Parallel High-Order Flow Solver for LES and DNS", 2002, 32nd AIAA Fluid Dynamics Conference, AIAA-2002-3123.
27. Visbal, M. R. and Gaitonde, D., "Direct Numerical Simulation of a Forced Transitional Plane Wall Jet", 1998, AIAA 98-2643.
28. Visbal, M. and Rizzetta, D., "Large-Eddy Simulation on Curvilinear Grids Using Compact Differencing and Filtering Schemes", 2002, ASME Journal of Fluids Engineering, Vol. 124, No. 4, pp. 836-847.
29. Rizzetta, D. P., and Visbal, M. R., 2001, "Large Eddy Simulation of Supersonic Compression-Ramp Flows", AIAA-2001-2858.
30. Spalding, D.B., "A single formula for the law of the wall", 1961, Journal of Applied Mechanics, Vol. 28, pp. 455.
31. Hunt, J. C. R., Wray, A. A., and Moin, P., "Eddies, stream, and convergence zones in turbulent flows", 1988, Proceedings of the 1988 Summer Program, Report CTR-S88, Center for Turbulence Research, pp. 193-208.
32. Dubief, Y., and Delcayre, F., "On coherent-vortex identification in turbulence", 2000, Journal of Turbulence, Vol. 1, Issue 1, pp. 1-22.
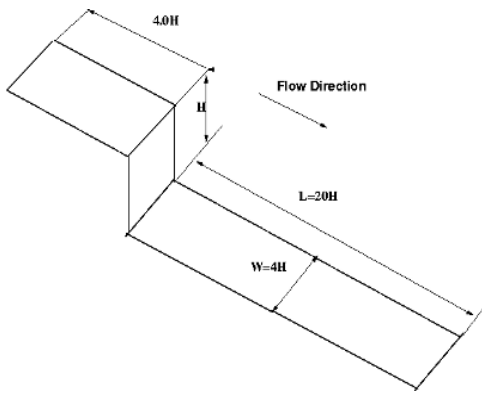
Figure 1 Schematic of the BFS configuration
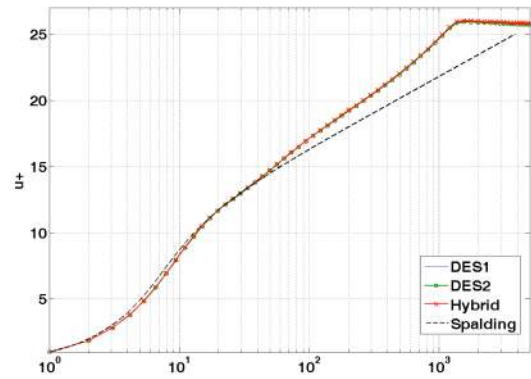
Figure 2(a) Time-mean spanwise averaged streamwise velocity profiles at the upstream region (X/H = 3.0) of the BFS
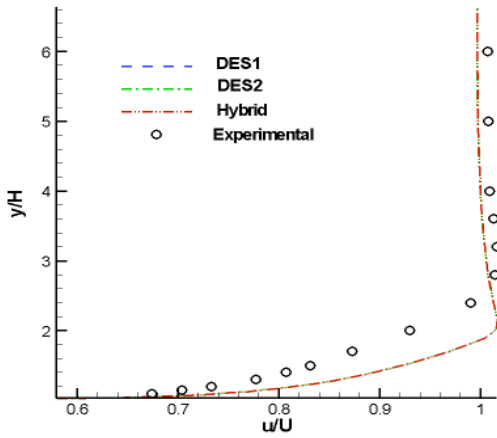
Figure 2(b) Time-mean spanwise averaged streamwise velocity profiles at the upstream region (X/H = 3.0): Comparison with experiment
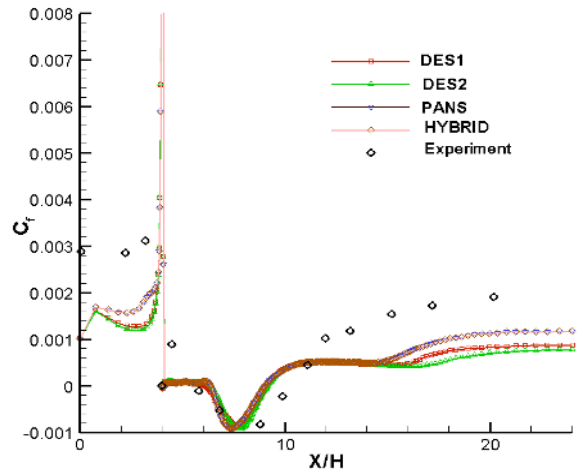
Figure 3 Time-mean span-wise averaged Skin Friction Coefficient Distribution over the backward facing step
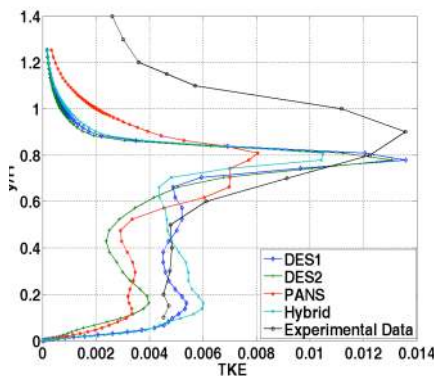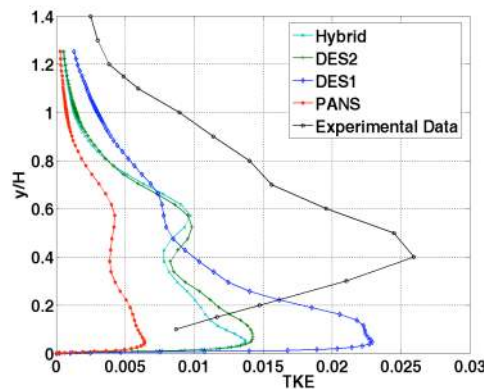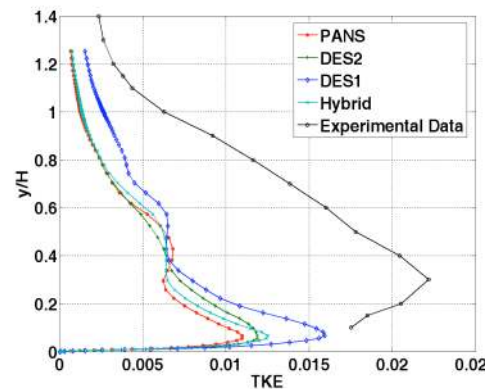
X/H = 5.5   X/H = 6.5   X/H = 7.5

Figure 4 Time-mean span-wise averaged grid resolved Turbulent Kinetic Energy (TKE) profiles for different models
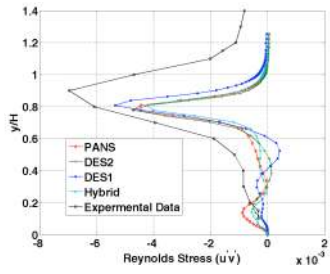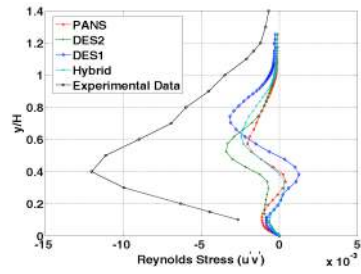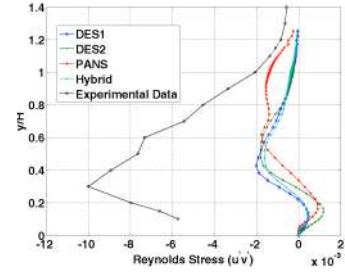
X/H = 5.5   X/H = 6.5   X/H = 7.5

Figure 5 Time-mean span-wise time averaged Reynolds Stress profiles for Backward Facing Step for different models
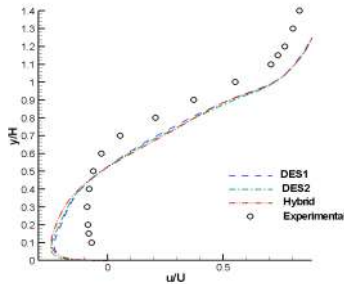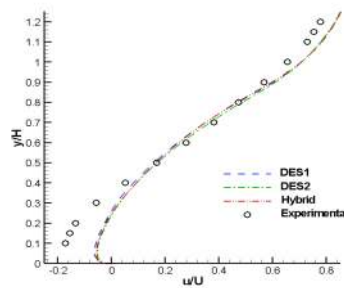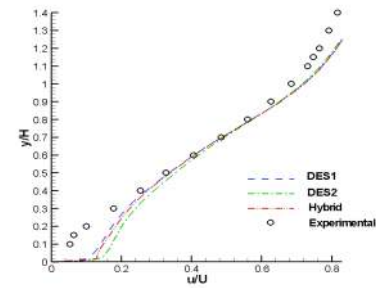
X/H = 5.0   X/H = 5.5   X/H = 7.0

Figure 6 Time-mean span-wise averaged streamwise velocity profiles for Backward Facing Step for different models
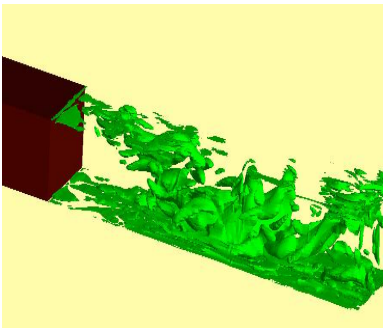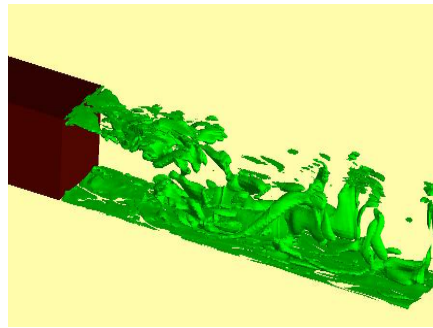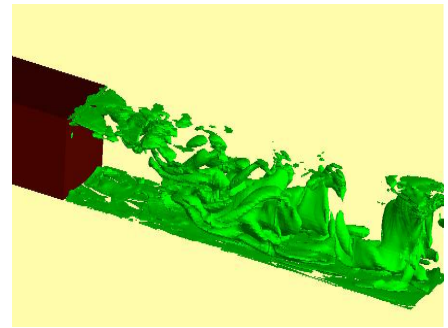
DES1   DES2   Hybrid

Figure 7 Iso-surfaces of the axial component of Q (Q_x) for the BFS flow for different turbulence models
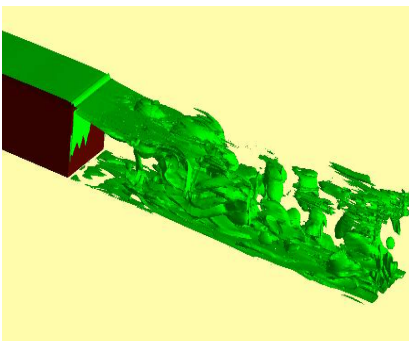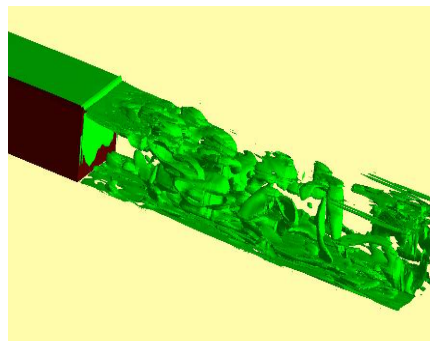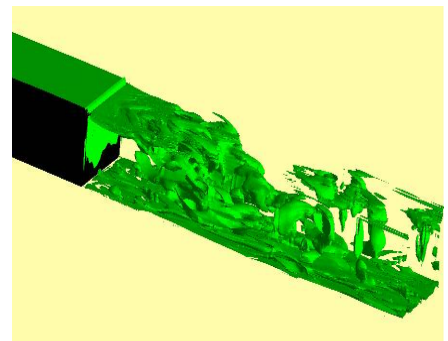
DES1   DES2   Hybrid

Figure 8 Iso-surfaces of the spanwise component of Q (Q_z) for the BFS flow for different turbulence models